JOURNAL OF GEOPHYSICAL RESEARCH, VOL. 106, NO. B6, PAGES 11,335–11,351, JUNE 10, 2001

BEDMAP: A new ice thickness and subglacial topographic model of Antarctica

Matthew B. Lythe,[1] David G. Vaughan,[1] and the BEDMAP Consortium

British Antarctic Survey, Natural Environment Research Council, Cambridge, United Kingdom

Abstract. Measurements of ice thickness on the Antarctic ice sheet collected during surveys undertaken over the past 50 years have been brought together into a single database. From these data, a seamless suite of digital topographic models have been compiled for Antarctica and its surrounding ocean. This includes grids of ice sheet thickness over the grounded ice sheet and ice shelves, water column thickness beneath the floating ice shelves, bed elevation beneath the grounded ice sheet, and bathymetry to 60°S, including the sub-ice-shelf cavities. These grids are consistent with a recent high-resolution surface elevation model of Antarctica. While the digital models have a nominal spatial resolution of 5 km, such high resolution is justified by the original data density only over a few parts of the ice sheet. The suite does, however, provide an unparalleled vision of the geosphere beneath the ice sheet and a more reliable basis for ice sheet modeling than earlier maps. The total volume of the Antarctic ice sheet calculated from the BEDMAP grid is 25.4 million km^3, and the total sea level equivalent, derived from the amount of ice contained within the grounded ice sheet, is 57 m, comprising 52 m from the East Antarctic ice sheet and 5 m from the West Antarctic ice sheet, slightly less than earlier estimates. The gridded data sets can be obtained from the authors.

1. Introduction

Mapping the topography of the Earth's surface has been a major preoccupation of geoscientists, surveyors, hydrographers, and cartographers for several hundred years [*Canadian Hydrographic Office*, 1981; *National Geophysical Data Center*, 1988], but in recent decades, satellite remote sensing and imaging depth sounders have added to their tools, and the majority of the surface of the geosphere is now mapped at high resolution [*Smith and Sandwell*, 1994; *Bamber et al.*, 1998; *Liu et al.*, 1999]. One part of the geosphere's surface has, however, remained beyond the reach of conventional or satellite methods: the bed beneath the great ice sheets of Antarctica and Greenland. Antarctica has been the subject of many local topographic compilations [*Jankowski and Drewry*, 1981; *Shabtaie et al.*, 1987; *Vaughan et al.*, 1994; *Steinhage et al.*, 2000], but there has been no coordinated effort to integrate all the existing data into a single topographic model of the entire continent.

Prior to this study, the most widely cited topographic representation of the bed beneath the Antarctic ice sheet was a folio of maps published by Scott Polar Research Institute (SPRI) [*Drewry and Jordan*, 1983; *Drewry*, 1983a, 1983b]. The SPRI Folio Series was produced by using data during surface traverses and airborne surveys, notably the campaign mounted by SPRI, the National Science Foundation (NSF), and the Technical University of Denmark (hereinafter SPRI/NSF/TUD) between 1967 and 1979. This campaign covered about one third of the continent at 100-km line spacing. Although contours of bed elevation were drawn over the entire continent with the exception of the Antarctic Peninsula, there were more than 500 km between measurements in many areas. The SPRI Folio Series was later digitized, on a 20-km grid, for large-scale modeling studies [*Budd et al.*, 1984], and versions of this are still widely used today [*von Frese et al.*,1999; *Bamber et al.*, 2000; *Huybrechts et al., 2000*]. With the exception of updates over limited areas, these data sets do not incorporate the large quantity of data collected over the past two decades.

In this paper, we present a suite of integrated digital topographical models for the Antarctic continent and its surrounding ocean, which incorporate all the available data from Antarctica. Our aim was to produce a self-consistent model, at sufficiently high resolution to provide a basis for meaningful, time-dependent ice sheet modeling. To this end, we designed an automated gridding scheme which relies on direct ice thickness measurements and other indirect supporting data. We aimed to honor the measurements where they exist and to produce a plausible representation where no data exist.

To facilitate modeling of the ice sheet through a complete glacial cycle, we extended the subglacial topography to 60°S, beyond the continental shelf edge, the probable limit of the ice sheet during recent glaciations. We seamlessly matched subglacial, bathymetric, and sub-ice-shelf topography.

The processing steps involved in the construction of the final digital elevation model (DEM) are shown in Figure 1. In summary, we produced an ice sheet thickness grid from the ice thickness measurements and several supporting derived data sets. This grid was then subtracted from the best available surface DEM [*Liu et al.*, 1999] to determine the bed beneath the grounded ice sheet. The resulting grid was then matched at the grounding lines with a compilation of the bathymetry. In the intervening region covered by ice shelves we used seismic data, where available, to control the configuration of bed topography.

Integration of all the source data required a consistent projection, geoid model and geographic framework. In accordance with the recommendations of the *Scientific Committee on Ant-*

Paper number 2000JB900449.
0148-0227/01/2000JB900449$09.00

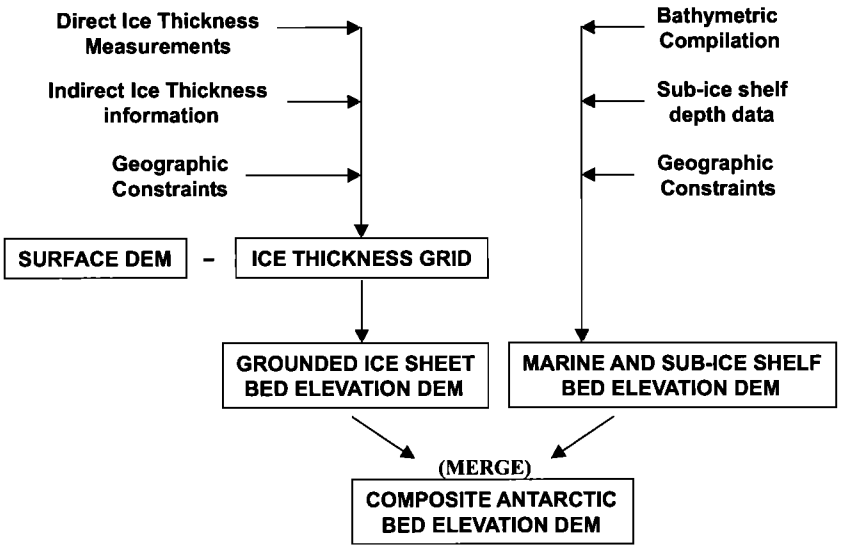

Figure 1. Processing steps involved in the construction of final bed elevation DEM.

arctic Research Working Group on Geodesy and Cartography [1961], we used the polar stereographic projection, with 71°S as the latitude of true scale and 0°E as the central meridian. A geopotential model, OSU91A [*Rapp et al.,* 1991], was chosen as the vertical reference system for integration of all the source data. The minor differences between mean sea level elevation and geoid orthometric height are expected to be 1.5 m on average [*Bamber and Bindschadler,* 1997] and so were ignored.

To delimit the continent and its physiographic elements (e.g., ice sheet, ice shelf, ice-free ground) (Figure 2a), we used the 1:1,000,000 scale data set from the Antarctic Digital Database (ADD) [*BAS et al.,* 1993]. This is the highest- resolution data set with coverage of the entire continent, and it provides descriptions of rock outcrop polygons, grounding lines, ice shelves, and ice rises. The ADD has a maximum error in horizontal position at this scale of around 300 m [*Fox and Cooper,* 1994].

The integration, manipulation, and generation of all products was carried out by using the ARC/INFO Geographic Information System (GIS), supplemented with customized data transformation, error correction, and interpolation functions.

2. Ice Thickness Model

2.1. Ice Thickness Data Compilation

In the 1950s and 1960s, only seismic and gravimetric methods were used to measure ice thickness. Collection of these data was laborious and could only be done at infrequent intervals on ground-based traverses. Gravity measurements are more rapid than seismic shooting, but to be useful, they must to be controlled by seismic or other data [*Robin,* 1971]. Nowadays, radio echo sounding enables faster acquisition of data by producing a continuous record of the bottom profile beneath the aircraft trajectory [*Robin et al.,* 1973].

The data assembled within the BEDMAP database derive from five types of measurement; airborne radar sounding, ground-based radar sounding, seismic refraction and reflection, gravimetric measurement, and drilling, with the majority gathered during ice-sounding radar programes. Since the data have been collected by different researchers using different techniques which have evolved considerably, assessment of data quality and the harmonization of all data sets required considerable effort.

2.1.1. Sources of ice thickness data. Data were obtained both from the literature and from unpublished surveys contributed to the BEDMAP Project by a consortium of institutes and investigators (Table 1). We included data from more than 150 independent surveys, conducted by 15 nations, over the past 50 years. The compilation includes over 1,400,000 km of airborne radar sounding profiles, around 250,000 km of ground-based radar and seismic traverse, and more than 5000 seismic reflection stations.

While considerable new data are available, the overall coverage is still patchy, as the surveys were undertaken in support of other scientific activities (Figure 2b). Although a few areas have dense data coverage with track-spacing of around 10 km (e.g., Amery Ice Shelf, Ronne-Filchner Ice Shelf, Siple Coast), the distance between tracks in other areas is over 50 km. There are several areas for which even reconnaissance level data have yet to be collected, (e.g., Queen Mary Land, Wilhelm II Land, coastal Marie Byrd Land, and the area of the polar plateau between the South Pole and 80°S and between 45°W and 10°E).

2.1.2. Ice thickness calculation. The reliability of ice thickness measurements determined by radar, seismic, and gravimetric techniques is contingent on assumptions specific to the method. For radar data, the greatest uncertainty results from the speed of radio waves in ice [*Drewry,* 1975]. No single value has been uniformly applied to all measurements; different workers have assumed mean speeds of between 168 and 171 m/μs. Additional sources of error arise through uncertainties in correcting for the low-density firn layer, where the speed of radio waves is considerably higher; corrections in the range of 10-15 m of ice thickness have been routinely applied. The methods of recording and digitizing field records can also introduce uncertainties. The assembled radar data have an estimated total measurement precision of between 1% and 5% of ice thickness.

For seismic measurements, the principal source of error arises from uncertainty in the wave propagation velocity, which is affected by variations in density, crystal size and orientation, and temperature [*Rothlisberger,* 1972]. Although the velocity does vary with depth, most researchers have used a constant value around 3.915 km s^{-1}. *Bentley* [1964] suggested an accuracy of 3% for ice thickness values from seismic shooting in Antarctica; however, misinterpretation of seismograms and mistakes in digitization can lead to larger errors.

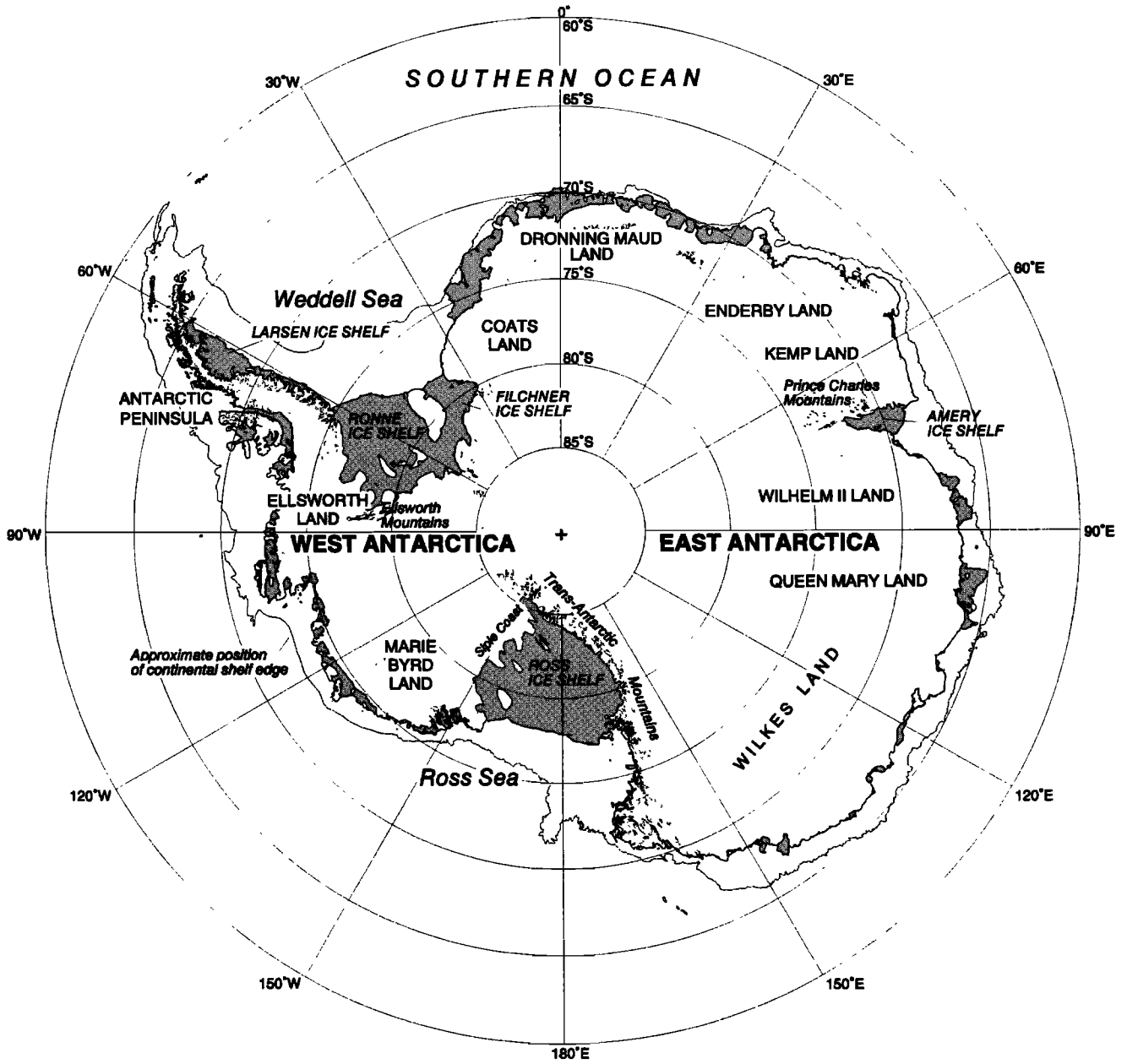

Figure 2a. Antarctic location map.

Gravity observations differ from others in that they yield an average thickness over a region rather than a point measurement. Uncertainty arises from instrumental drift and calibration but is primarily due to the assumptions regarding geological properties and terrain correction factors. *Kapitsa and Sorokhtin* [1963] suggest an average accuracy of 7-10% for gravimetric ice thickness measurements, but errors of 15-20% are likely in areas of complex bed topography.

In compiling the BEDMAP database we accepted the values of ice thickness supplied by contributors and from the published data but stored what information is available concerning the corrections alongside the data for each mission. We have not attempted to recalculate values by using standard assumptions, as the raw data were not always available.

2.1.3. Navigation. Since the late 1980s most geophysical surveys have been navigated by using Global Positioning Systems (GPS) and are thus well fixed with respect to an ellipsoidal reference framework. Navigation methods employed prior to GPS such as celestial navigation, inertial avionics (INS), Doppler avionics, traditional survey, and dead reckoning have far larger uncertainties. For example, the positional error for traverse data navigated by using astronomical and solar observations are approximately 2-3 km, while the SPRI/NSF/TUD radar soundings using inertial navigation systems are only accurate to ~5 km [*Drewry,* 1983a]. Of the assembled data, around 50% are positioned with GPS, 25% with INS, 11% with traditional survey and about 8% with Doppler avionics.

In addition to the navigational uncertainty, several of the data sets were fixed to maps which had inaccurately located geographic features. Our analysis has shown (see "Crossover analysis") that while refixing of the navigational data might be possible, using known positional fixes or even using a random walk technique, this is not required for the present generation of continent-scale topographic models and so is not attempted in this study.

2.1.4. The BEDMAP database. The BEDMAP database

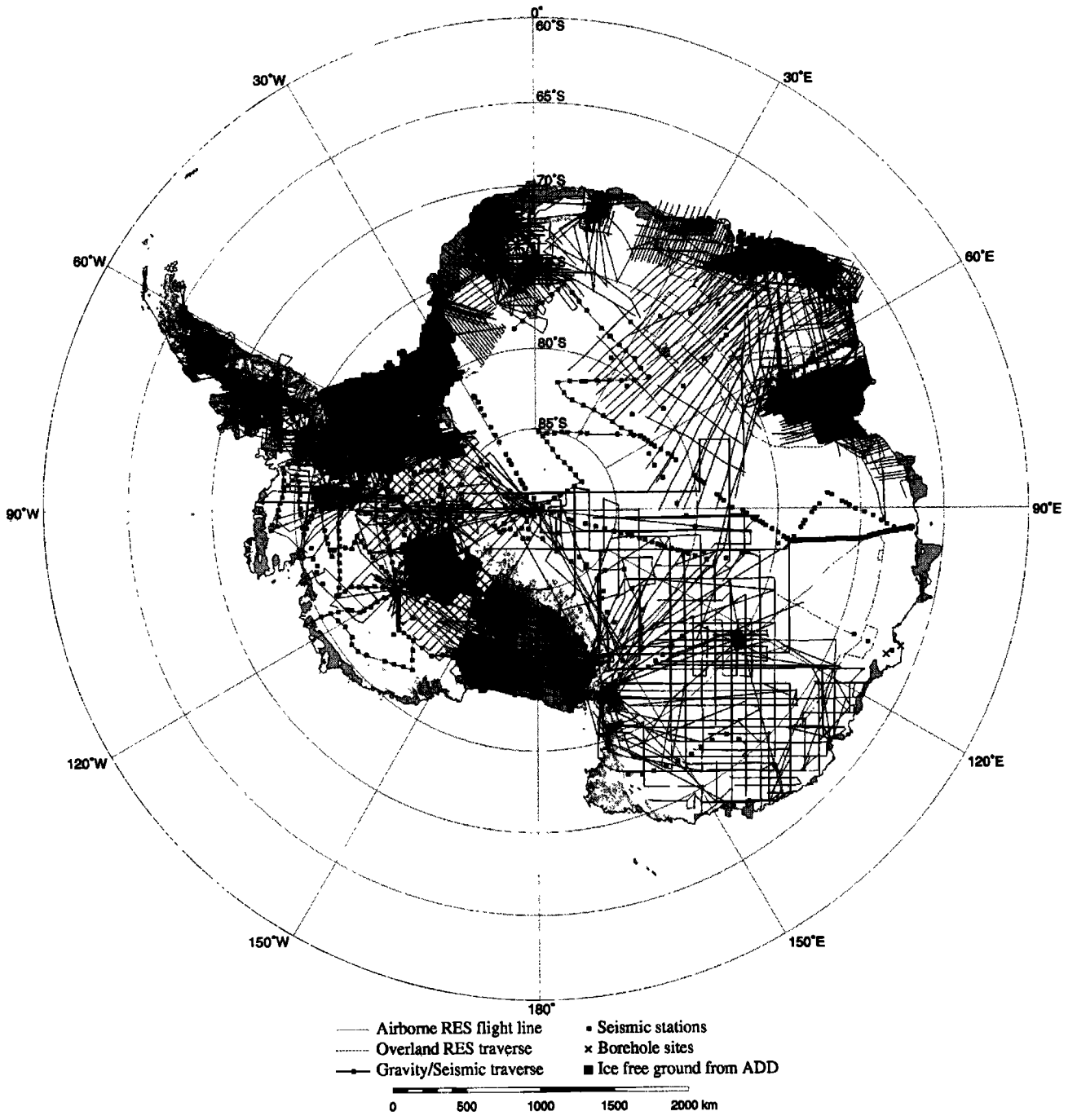

Figure 2b. Distribution of ice thickness data in the BEDMAP database.

currently includes around 2,500,000 direct measurements of ice thickness, an estimated 90% of all data collected over the Antarctic ice sheet to date. The outstanding data include surveys undertaken during the past 2-3 seasons, and a small quantity of old data which are, to our purposes, lost. The data are divided into missions, which represent data collected during one or several consecutive field seasons by one scientific party using consistent techniques. The data were consolidated, with accompanying documentation for each mission, in a relational database housed at the British Antarctic Survey (BAS), Cambridge, UK.

For the majority of data sets we have compiled only the derived parameters, surface elevation, ice thickness, bed elevation, and water column thickness. Data have been contributed on the basis that they remain under the control of the contributing institutes; thus access restrictions remain on a number of data sets.

2.2. Construction of Ice Thickness Model

The primary data used in the construction of the ice thickness model were direct ice thickness measurements, but we also used rock outcrop polygons, which approximate to isopleths of zero mean ice thickness, and ice shelf thickness determined by hydrostatic conversion of surface altimetry.

Even with these additions the total coverage was, however, too sparse to generate a reasonable model over the entire continent. For this reason, we designed other fields to help control the gridding in areas where the data were sparse and in mountainous

Table 1. Sources, Survey Types, and Dates for Ice Thickness Data Collected Over Antarctica and Compiled in the BEDMAP Database

Institute	References	Data Type	Years
Instituto Antártico Argentino	*Keller et al. [1990]*	S	1988-1991
Australian Antarctic Division/ Antarctic CRC	*Walker* [1966], *Budd et al.* [1982], *Allison et al.* [1982], *Morgan et al,* [1982], *Young et al.* [1989], *Higham et al.* [1995]	A,B,G,O,S	1957-1998
University of Brussels, Belgium	*Dieterle and Peterschmitt* [1964], *Autenboer and Decleir* [1978], *Pattyn and Decleir [1995]*	A,G,O,S	1959-1992
Universidad de Chile	*Casassa et al* [1998]	O	1997-1998
Alfred-Wegener-Institut, Germany	*Steinhage et al* [2000]	A	1994-1999
Universität Munster, Germany	*Hoppe and Thyssen* [1988]	A	1985-1990
Bundesanstalt fur Geowissenschaften und Rohstoffe, Germany	*Damm* [1996]	A	1992-1996
Universitá degli Studi di Milano, Italy	*Tabacco et al.* [1998]	A, O	1992-1998
National Institute of Polar Research, Japan	*Ageta et al.* [1987], *Nishio et al.* [1986]	O	1969-1997
Arctic and Antarctic Scientific Research Institute, Russia	*Kapitsa* [1964], *Macheret et al.* [1997]	S, G	1956-1964
Ministry of Natural Resources of the Russian Federation, Polar Marine Geological Research Expedition	*Pozdeev and Kurinin,* [1987], *Kurinin and Aleshkova* [1987]	A, S	1970-1996
Russian Academy of Sciences, Russia	*Macheret et al* [1997]	O	1995-1997
British Antarctic Survey, Cambridge, UK	*Johnson and Smith* [1997], *Smith and Doake* [1994]	A, G, O, S	1951-1999
Scott Polar Research Institute, National Science Foundation, Technical Univ. Denmark	*Drewry* [1975], *Drewry and Jordan* [1983], *Jankowski and Drewry* [1981]	A	1969-1979
University of Wisconsin - Madison	*Behrendt* [1962]; *Crary et al.* [1962], *Retzlaff et al.* [1993]	A,S	1957-1988
University of Washington, Seattle	*Gades et al.* [2000]	A	1996-1997
St. Olaf College, Northfield, Minnesota	*Jacobel et al* [1996]	O	1995-1996
The University of Texas, Austin	*Blankenship et al* [2000]	A	1991-1996
University of Alabama, Tuscaloosa	*Anandakrishnan et al.* [1998]	S	1996-1997

[a]Sources, survey types, and dates for ice thickness data collected over Antarctica and compiled in the BEDMAP database. The legend for the survey type is as follows: A, airborne radio-echo sounding (RES); O, over-snow RES, S, seismic; G, gravity; B,- borehole.

regions, These fields rely on a priori assumptions and are derived from regression models, and while they do not represent the true ice thickness, they produce a plausible surface and help to reduce the appearance of artefacts caused by data sparsity. We added one further control: by defining the longitudinal profile of the large outlet glaciers in East Antarctica which are important as outlets for ice from the interior ice sheet, we used a linear interpolation of ice thickness at the grounding line to the nearest upstream measurement to ensure that they were represented in the final model.

Finally, the combined data sources were used as input into a specifically designed spatial interpolation algorithm which is described below.

2.2.1. Data preprocessing. The ice thickness measurements include inherent uncertainties, and to extract a reliable set of observations for the gridding, we carried out some data preprocessing. The goal was to flag erroneous values within the database and reduce the data set before interpolation. The data preprocessing was carried out in three steps.

2.2.1.1. Crossover analysis: Crossover analysis provides an estimation of the overall integrity and precision of the data set. Here a crossing point was defined where two observations from separate missions or separate flights within the same mission were separated horizontally by 500 m or less. From around 16,000 crossing points we found a root-mean-square (RMS) difference in ice thickness of 156.2 m and a median absolute (MA) difference of 21 m. The distribution of crossover errors has a sharper peak and longer tail than a normal distribution.

The distribution of the absolute crossover errors (Figure 3) reveals that around 58% of crossover errors are less than 20 m, 73% are less than 50 m, and 84% are less than 100 m. This indicates that the majority of crossover errors fall within typical navigational and measurement uncertainties. The long-tailed distribution suggests there is a small percentage of large crossover errors, but neighborhood variance checks (described below) suggest that a program of extensive flight line refixing was not required. Refixing was, however, carried out on a few flight lines where clear errors in track position existed.

2.2.1.2. Data reduction: The majority of ice thickness data have been collected by using airborne radio echo sounding (RES) techniques, a method that results in highly anisotropic data distribution; i.e., the data are densely sampled along track while the flight tracks themselves are widely spaced. The SPRI/NSF/TUD data, for example, have a typical along-track spacing between samples of 1-2 km and an across-track separation of 50 km. Such a distribution poses serious difficulties for most interpolation techniques and results in a directional bias in the grid. To counter this, we used a filter to reduce the high-density track line data, but before this, we preprocessed the data to identify and remove isolated erroneous data points.

In the preprocessing step, a seven-point filter was applied to each track-line. The mean ice thickness, standard deviation, and along-track spread of the seven data points were calculated. If the along-track spread was greater than 6 times the mean ice thickness, the data were regarded as insufficiently dense for filtering. If the spread was less than 6 times the mean ice thickness and the central observation within the window differed by more than twice the standard deviation, that observation was removed. This procedure proved effective in removing around 1500 spikes from the track line data.

In the data reduction phase, new data points were established along the profile with a spacing of 2500 m. These new sample nodes were then assigned the median ice thickness of observations within 2500 m along that profile. The median value was used instead of the mean value to avoid unnecessary smoothing and to ensure that the value assigned was an actual observed value. Where data was highly anisotropic, with track spacing greater than 50 km, we filtered the data by using a 5000-m sample spacing.

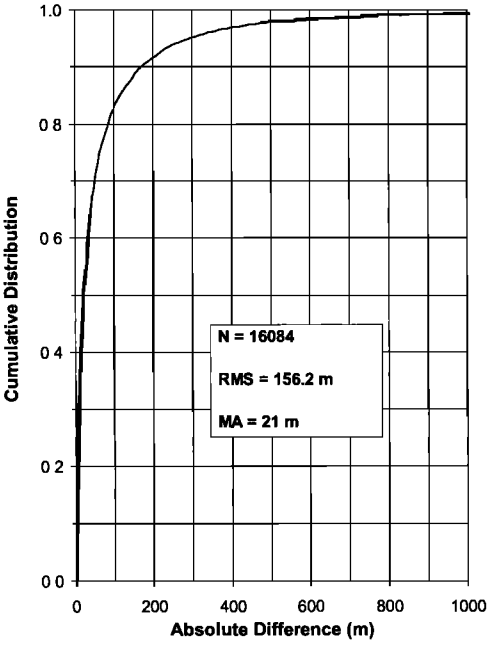

Figure 3. Cumulative distribution of crossover errors in ice thickness measurements.

While this procedure removed legitimate high-frequency information along the track, particularly on the very densely spaced data, the resulting profiles depict the variation in ice thickness over a wavelength nearer the resolution of the final grid. This reduced the problems associated with anisotropic data distribution. Approximately 2 million data points from both anisotropic airborne and ground-based track line data were filtered by using this procedure, leaving a reduced data set of around 160,000 data points, significantly reducing processing time required for the spatial interpolation.

2.2.1.3. Neighborhood variance check: In general, ice sheet thickness is a parameter exhibiting a high degree of spatial autocorrelation. The correlation length indicates the distance or range of spatial dependence and varies across the ice sheet. The semivariogram expresses mathematically changes in variance with distance and direction between any two points [*Cressie and Hawkins*, 1980]. Semivariograms indicate the nature of autocorrelation in different parts of the ice sheet.

Three parameters define the semivariogram: the nugget, the measurement error and natural variance for nearby measurements; the sill, the variance of the data set beyond the range of spatial correlation; and the range, the distance beyond which spatial correlation is insignificant. The relative nugget effect (ratio of nugget to sill) gives an indication of the level of spatial dependence described by the semivariogram model.

The semivariograms (Figure 4) show that spatial autocorrelation is large over both the interior ice sheet and the Ross Ice Shelf. In mountainous regions, large changes in ice thickness occur over short distances, and the autocorrelation is much lower. The high nugget value and large relative nugget effect (0.86) in the Trans-Antarctic Mountains show that over distance greater than around 40 km, ice thickness is not a regionalized

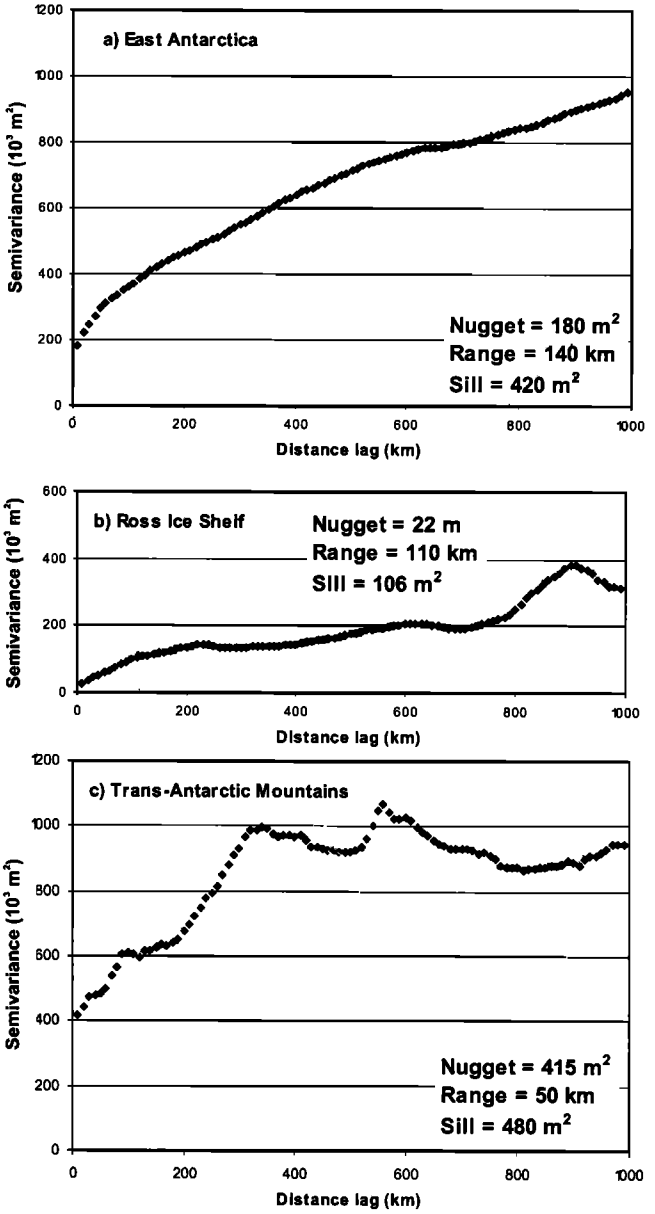

Figure 4. Geostatistical properties of the ice thickness data in (a) East Antarctica, (b) Ross Ice Shelf, and (c) Trans-Antarctic Mountains.

variable. Over the ice shelves and interior ice sheet, relative nugget effect values of 0.19 and 0.23, respectively, show good spatial autocorrelation. This principle provides the basis for our final quality control procedure, a neighborhood variance check.

We identified crossing points defined where two observations from separate flights were separated by less than 1000 m. Of these, crossovers with an absolute value greater than 100 m were flagged as potentially in error. Around 15,000 data points were identified from this procedure.

For each of these data points we established a localized neighborhood, defined as all points within a radial distance of 5000 m. The variance characteristics (mean and standard deviation) of all other observations within this neighborhood were then determined. Providing the neighborhood contained at least five measurements, if the value of the central observation was greater than twice the standard deviation different from the neighborhood mean, it was flagged as unreliable and removed from the interpolation data set. Of the points flagged as potentially anomalous, just over 1000 (~7%) were removed by using this procedure. After the removal of these observations, the overall RMS error of all remaining crossover points dropped from 156.6 to 134.2, justifying the preprocessing step.

The preprocessing described above yielded a final set of ~200,000 ice thickness data points, comprising approximately 160,000 data points from the reduced track line data and around 40,000 other ice thickness measurements.

2.2.2. Rock outcrops. Approximately 0.3% of the Antarctic continent is free of ice for at least part of the year [*Fox and Cooper,* 1994]. These areas of permanent rock outcrop are a valuable source of information for the ice thickness model. Here we used rock outcrop polygons from the 1:1,000,000 scale ADD: a total area of approximately 50,000 km²; over 75% have an area of less than 1 km² and only 250 have an area of greater than 5 km². Thus most of the outcrops are much smaller than the resolution of the final grid we chose to depict ice-free ground as point data, allowing us to use them in the same manner as other measurements of ice thickness.

The conversion of the polygon data to point observations was carried out by using a two-stage procedure. First, we extracted from all outcrops the polygon centroids. These provide an adequate representation of the small nunataks. Second, we selected outcrops with an area greater than 25 km² (the size of a single grid cell in final model) and extracted a set of vertices spaced at 2 km around the polygon perimeter. The resulting nodes provided a reasonable description of the extent of the larger ice-free areas. This procedure ensures that extensive outcrops are adequately represented, while nunataks smaller than the grid spacing were not disproportionately represented.

2.2.3. Hydrostatic conversion for floating ice. Over distances greater than a few times the ice thickness, ice cannot support significant vertical shear stresses for more than a few years [*Casassa and Whillans,* 1994]; consequently, floating ice shelves are generally in regional hydrostatic equilibrium. The total ice thickness or draft is related to the surface elevation by the following relation [*Jenkins and Doake,* 1991]:

$$h = \frac{\rho w - \rho i}{\rho w} H + \frac{\rho i}{\rho w} d + e, \qquad (1)$$

where h is the freeboard with respect to the ellipsoid; H is the thickness of the ice shelf; ρ_W and ρ_I, are the mean densities of the seawater and ice, respectively; d is the thickness of the air-fraction contained in the low-density upper layers; and e is the geoid/ellipsoid separation.

This relationship is linear if constant densities are used. While the density of water beneath the shelf is relatively constant (1028-1032 kg m^{-3}), the density of ice may vary owing to (1) difference in the densification rate of the firn layer, (2) freeze-on of marine ice to the base of the shelf, or (3) crevassing. This relationship has been widely used [*Budd,* 1966; *Thyssen and Grosfeld,* 1988]. The slope varies with density characteristics of the ice, while the intercept value represents a correction for the low-density firn and offsets in the geoid model from sea level.

Analysis of the regression models developed for different ice shelves shows that the total variation between models is approximately 10 m, mostly arising from the different densities used. This error envelope suggests that this conversion provides a useful additional source of ice thickness data over unsurveyed or data-sparse ice shelves. The value of the method is increased because radar sounding is unable to measure total ice thickness in areas which contain a marine ice layer or exhibit crevassing

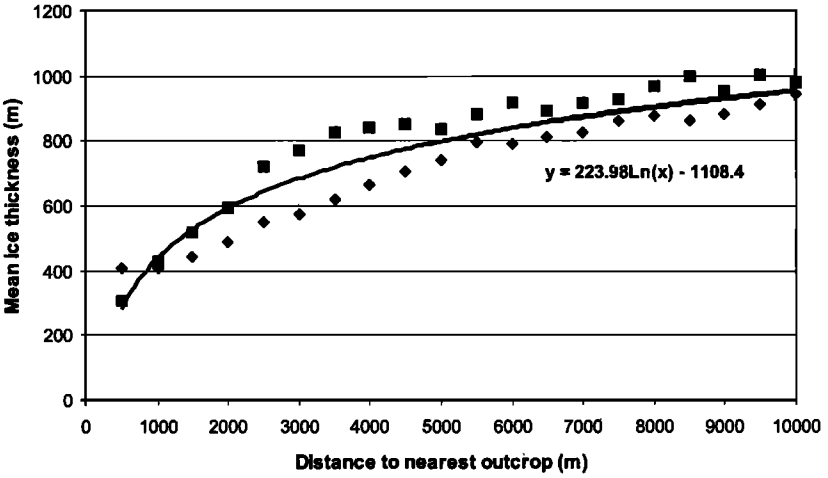

Figure 5. Thin ice regression models developed from data in Prince Charles Mountains (diamonds) and Dronning Maud Land (squares). The line indicates the thin ice model dervied from all data within 10 km of ice- free ground in both areas.

[*Vaughan et al.*, 1995] such as the Filchner-Ronne Ice Shelf (FRIS) and the Amery Ice Shelf, which are known to contain significant marine ice layers [*Englehardt and Determann*, 1987; *Morgan*, 1972].

We have determined total ice thickness for data-sparse ice by using a hydrostatic conversion model applied to a high-resolution Antarctic DEM [*Liu et al.*, 1999]. Over FRIS and other ice shelves where surface crevassing is apparent, data derived in this way were used in preference to radar measurements. Points were determined on a regular 2-km grid. A single model,

$$h = 0.108H + 16, \quad (2)$$

was used with a slope based upon a mean density for ice of 917 kg m^{-3} and water of 1028 kg m^{-3}. A constant intercept value of 16 m was used for all regions to account for the lower firn density of the upper ice layer and geoid/ellipsoid separation. Data points within 10 km of grounded ice were not included.

To validate this conversion, we determined the cross-correlation coefficient ($r^2 = 0.91$) between measured ice thickness and thickness derived from hydrostatic conversion, [for all seismic data more than 10 km from grounding ice.]

2.2.4. Thin ice model. In some mountainous areas (e.g., Antarctic Peninsula, Victoria Land, and Dronning Maud Land), there are few measurements of ice thickness. Many glaciers, névés, and basins have not been sounded at all. Here rock outcrops are the only source of ice thickness data, and the measurements are thus heavily biased toward zero ice thickness. Without some further control, we would produce a grid in which most of the mountainous areas were represented as entirely ice free.

To produce a more plausible model in these data-sparse regions, we developed an empirical regression model where ice thickness is related to the distance to the nearest exposed rock (Figure 5). The results show that within 10 km of outcrops there is a good correlation between ice thickness and outcrop distance. This model provides a more plausible solution for mean ice thickness in data-sparse regions containing exposed rock, although this thin ice model still underestimates ice thickness in these areas.

The thin ice model was used to generate ice thickness data on a regular 10-km grid in regions where exposed rock outcrops were the principal source of data. These include the Antarctic Peninsula, Trans-Antarctic Mountains, Coats Land (Theron Mountains), Dronning Maud Land, and Marie Byrd Land.

2.2.5. Outlet glaciers. Fast-flowing glaciers, which drain much of the Antarctic ice sheet, must be resolved if we are to produce reliable models of the ice sheet [*Payne*, 1997, 1999]. Many such glaciers, particularly those bordered by rock outcrop (outlet glaciers), which have not been sounded, would not naturally appear in our grid. We have ensured that some representation of these features remains, by including "manufactured" ice thickness data along their length. This method was applied to the major outlet glaciers which did not have measured profiles (Table 2). For these features, we derived ice thickness data along their centerline by linear interpolation from the ice thickness at the grounding line to the closest measurement in the upper basin of the glacier.

Table 2. East Antarctica Outlet Glaciers for Which "Manufactured" Data Are Included in the Ice Thickness Model

Glacier	Grounding Line Position	Profile Length, km
Beardmore	171.604°E , 83.594°S	152.6
Nimrod	162.512°E , 82.374°S	159.2
Mulock	160.818°E , 79.138°S	146.1
Skelton	162.289°E , 78.969°S	101.8
Ferrar	163.530°E , 77.688°S	106.4
Mackay	162.296°E , 76.973°S	51.8
Mawson	162.422°E , 76.204°S	104.9
Priestly	163.453°E , 74.485°S	114.7
Campbell	164.334°E , 74.530°S	121.9
Aviator	165.096°E , 73.923°S	106.8
Mariner	166.714°E , 73.011°S	84.1
Lillie	163.923°E , 70.765°S	202.4
Rennick	161.802°E , 70.657°S	256.0

2.2.6. Continentality model. Finally, to produce a continuous surface for the entire ice sheet, we generated a set of manufactured ice thickness data points on a regular 50-km grid in the large data-sparse areas in Wilhelm II Land, Queen Mary Land, Coats Land, and Marie Byrd Land. To provide some plausible control in these regions, we used a continentality model derived by *Vaughan and Bamber* [1998]. This model relates the ice surface elevation/ice thickness to the distance from the grounding line.

2.2.7. Choice of grid spacing. We chose to present the gridded ice thickness and bed elevation on a regular grid at 5-km resolution for two principal reasons. First, most applications require a regular grid of base data, and so presenting the data in any form other than a grid would invite users to grid the data by whatever algorithm was available to them. Second, 5 km is sufficient to resolve ice streams and major outlet glaciers, and those features much be reproduced by any realistic ice sheet model. Finally, there are some areas where the data are dense enough to support this resolution, although we do emphasize the proviso that there are wide areas within the grid where the data available are not strictly sufficient to justify even a 100-km grid.

2.2.8. Spatial interpolation. Most spatial interpolation algorithms embody a model of continuous spatial change that can be described by a mathematically defined surface. The optimum algorithm for an application should be chosen according to whether input data points are to be honored exactly, how smooth and continuous the output surface is to be, and how weightings should be applied.

For the purposes of ice sheet modeling it is important that the final bed DEM incorporates local-scale variation where it is known, while also providing a smooth continuous surface. We considered several algorithms including triangulation, bicubic splines, moving averages, and geostatistical methods. While all of these methods performed reasonably well in areas of well-distributed data, their performance was poor where there were substantial gaps between observations or anisotropic data distribution.

The estimation procedure embodied in geostatistics, known as kriging, showed promise, but it is heavily reliant on the choice of semivariogram which expresses mathematically the way variance changes with distance between observations. We were unable to adequately fit a single semivariogram to suit the entire interpolation area (Figure 4). We could have used several semivariogram models for different regions, but this would have required the mosaicing of regional grids to produce a final continental grid.

To cope with the variable data density, irregular distribution and anisotropy, we developed an inverse distance weighting (IDW) algorithm that determines estimates by using an octagonal search neighborhood similar to the quadrant search used by *Liu et al.* [1999]. The IDW algorithm uses the nearest two observations in each octant (a total of 16 data points) to estimate the value at each grid node. This avoided the directional bias that results from a nearest-neighbor search, while mitigating the effects of data clustering and anisotropy by assigning equal weights to each sector. Observations within a search radius of 100 km were used in the estimation of each grid node. This distance was chosen as a mean correlation length in the semivariogram derived for several parts of the ice sheet. After considerable testing we found that inverse-cubed weighting produced the most plausible surface given the data distribution. This weighting reduces the influence of observations further away from the estimation point. The grid of ice sheet thickness is shown in Plate 1.

2.3. Uncertainty in the Ice Thickness Grid

Ideally, validation of the model requires comparison with an independent "true" surface, but in the absence of such a data set, we adopted a "jackknife" procedure. In jackknifing, truncated data sets are created by selectively removing samples from the original data. The statistics are then recalculated for each truncated data set and the variability among the original samples is used to describe the variability of the model [*Tichelaar and Ruff*, 1989].

We removed a randomly selected set of 5% of the data and regenerated the grid by using the remaining data. The deleted 5% (around 10,000 points) were then used to test the output grid. The median absolute difference between observed and predicted ice thickness was 41 m, while the RMS error of the jackknife resample was 152 m. As with the crossover errors, the RMS error is exaggerated because of occasional large errors. The cumulative distribution of absolute differences revealed that 70% of errors are less than 50 m and around 86% are less than 150 m.

This statistic, however, provides only a single measure of dispersion; it tells us nothing about the spatial variation in error across the grid. To quantify error in different parts of the model we determined the RMS error of the jackknife sample in different regions (Table 3). The results show that the magnitude of error reflects the frequency and amplitude of topographic variation. Over the ice shelves the frequency and magnitude of ice thickness variation are relatively low, compared with the Antarctic Peninsula or the Trans-Antarctic Mountains, where large changes in ice thickness occur over short horizontal distances. The errors in these areas reflect the inability of the model to incorporate subgrid-scale variation. It should be noted that the octagonal IDW interpolation procedure is by definition a smoothing technique, designed to estimate the mean ice thickness in a local neighborhood. The model therefore is representative only of topographic variations greater than 5 km.

3. Bed DEM

The construction of the bed DEM was completed in three stages with a different procedure being used for the grounded ice sheet, the sub-ice-shelf seabed, and the continental shelf/Southern Ocean seabed (Figure 1). In summary, the ice sheet thickness grid was subtracted from the best available surface DEM and then matched at the grounding line with a compilation of the adjacent ocean floor. Where seismic data were available, they were used to determine the bed topography beneath ice shelves.

3.1. Subglacial Bed DEM

While surface elevation was routinely measured at the same time as ice thickness, e.g., by barometric leveling, those measurements were of variable, often poor, quality and were sometimes subject to unrepeatable postprocessing. Thus we discarded the original surface elevation measurements in favor of using a single consistent surface DEM for the determination of bed elevation over the grounded ice sheet. Using separately constructed surface DEM and ice thickness grids, we can ensure consistency between the three parameters surface elevation, ice thickness, and bed elevation. This has the added advantage of enabling easy update of the bed DEM when future improvements are made to the surface DEM's.

We chose to use a recent high-resolution surface DEM of the Antarctic [*Liu et al.*, 1999], hereinafter the Liu-DEM, which in-

Table 3. Regional Variation in Confidence Limits of Ice Thickness Model Resulting From the Jackknifing Procedure

Region	Median Absolute Difference, m	RMS Error, m
East Antarctica interior ice sheet	59	153
West Antarctica	43	136
Ross Ice Shelf	4	18
Amery Ice Shelf	21	101
Antarctic Peninsula	57	163
Trans-Antarctic Mountains	138	332
Prince Charles Mountains	111	204

tegrates satellite altimetry, airborne altimetry, digital cartographic data, and ground survey data referenced to the OSU91A geoid. Absolute vertical accuracy varies across the Liu-DEM depending on the source data used in its construction. For the ice shelves it is around 2 m, over the interior ice sheet it is better than 15 m, in the steeper ice sheet perimeter it is 35 m, and over the rugged mountains it is approximately 100-130 m [*Liu et al.*, 1999]. It should be noted that in some of the mountainous regions, e.g., Antarctic Peninsula, the vertical accuracy of the Liu-DEM is more than 250 m, as it is based on estimated form lines (A. Cooper and J. Thomson, personal communication, 1999).

3.2. Bathymetry

The probable limit of grounded ice during the Quaternary was the edge of the continental shelf. We chose to extend the subglacial topography to 60°S to include all of the Antarctic continental shelf, so that our bed DEM would be useful for ice sheet modeling through glacial cycles.

Bathymetric data coverage in the Antarctic region is far from satisfactory, and many of the available charts are inconsistent [*Angrisano*, 1995]. In some, particularly south of 60°S, there are hundreds of kilometers between shipboard depth-sounding tracks, and much of this was collected by using celestial navigation; discrepancies in depths reported at crossover points exceed 100-250 m at half the track intersections [*Smith*, 1993]. While there is a need for a new model that integrates improved coastline data and all new soundings, it was not within the scope of this program to generate such a product. We have thus developed a bathymetric model south of 60°S which integrates several important bathymetric compilations. This is not intended to be a definitive bathymetry; rather, one that is consistent and integrates with the subglacial topography presented here.

3.2.1. Satellite altimetry and ship measurements. Radar altimeters aboard the ERS1 and GEOSAT spacecraft have been used to survey the marine gravity field over most of the world's oceans to a high accuracy and moderate spatial resolution (track spacing of 2-4 km). Over intermediate wavelengths (15-200 km), variations in gravity anomaly are highly correlated with seafloor topography if sediment cover on the ocean floor is thin [*Smith and Sandwell*, 1994]. Long-wavelength (greater than 160 km) topography is isostatically compensated and is not correlated with the gravity field. There are ongoing efforts to combine ship and satellite data to form a uniform resolution grid of seafloor topography [*Sichoix and Bonneville*, 1996; *Smith and Sandwell*, 1994, 1997].

We have used the predicted seafloor topography by *Smith and Sandwell* [1997] in this compilation. In the generation of this satellite gravity field and available depth measurements were used to determine the correlation between gravity and the seafloor topography. The vertical accuracy of this inferred data set is around 250 m [*Smith and Sandwell*, 1997]. Although the satellite altimetry data extended to 81.5°S this solution was carried only to 72°S because of concerns about ice problems (W. H. Smith, personal communication, 1999). The grid spacing is 3 min of longitude by 1.5 min of latitude.

3.2.2. Bathymetric chart of the Weddell Sea. The most accuarete bathymetric data set for the Weddell Sea is the Bathymetric Chart of the Weddell Sea (BCWS) [*Schenke et al.*, 1998] The charts cover the region from 66°S to 78°S and from 68°W to 0°E, and because of the lack of observations for ice covered areas, supplementary geophysical and geographical information was also included. Over the majority of the model the depths are accurate to within 50 m. Matched to this data set, west of the Antarctic Peninsula is a gridded data set compiled from published and unpublished soundings (P. Morris, personal communication, 1999).

3.2.3. Earth Topography 5. South of 72°S (excluding the Weddell Sea) where compilation derived from satellite-altimetry are not available, we integrated the Earth Topography 5 arc minute grid (ETOPO-5) [*National Geophysical Data Center*, 1988].

3.2.4. Model generation. The derived seafloor topography, BCWS, and western Antarctic Peninsula data sets were resampled onto a 5-km grid by using a cubic convolution filter. These data sets were then merged with the ETOPO-5 data set by using a Hermite cubic method in overlapping areas. The Hermite cubic is a proximity analysis algorithm that takes the input grids and calculates an output value area based on the normalized distance of the width of the overlapping area.

3.3. Sub-ice-shelf Topography

The sub-ice-shelf region of the seabed is inaccessible to both ship-sounding or airborne radar. Generally, only seismic soundings from the ice shelf surface can provide the seabed depth beneath an ice shelf, and seismic measurements are only available over a few ice shelves. Where no seismic data were available, we have used a bicubic spline to interpolate the seabed surface between the grounding line and the seabed at the ice front. Where seismic data were present, principally over the Ross, Filchner-Ronne, Larsen, and Amery Ice Shelves, we used the octagonal IDW algorithm described previously (with a re-

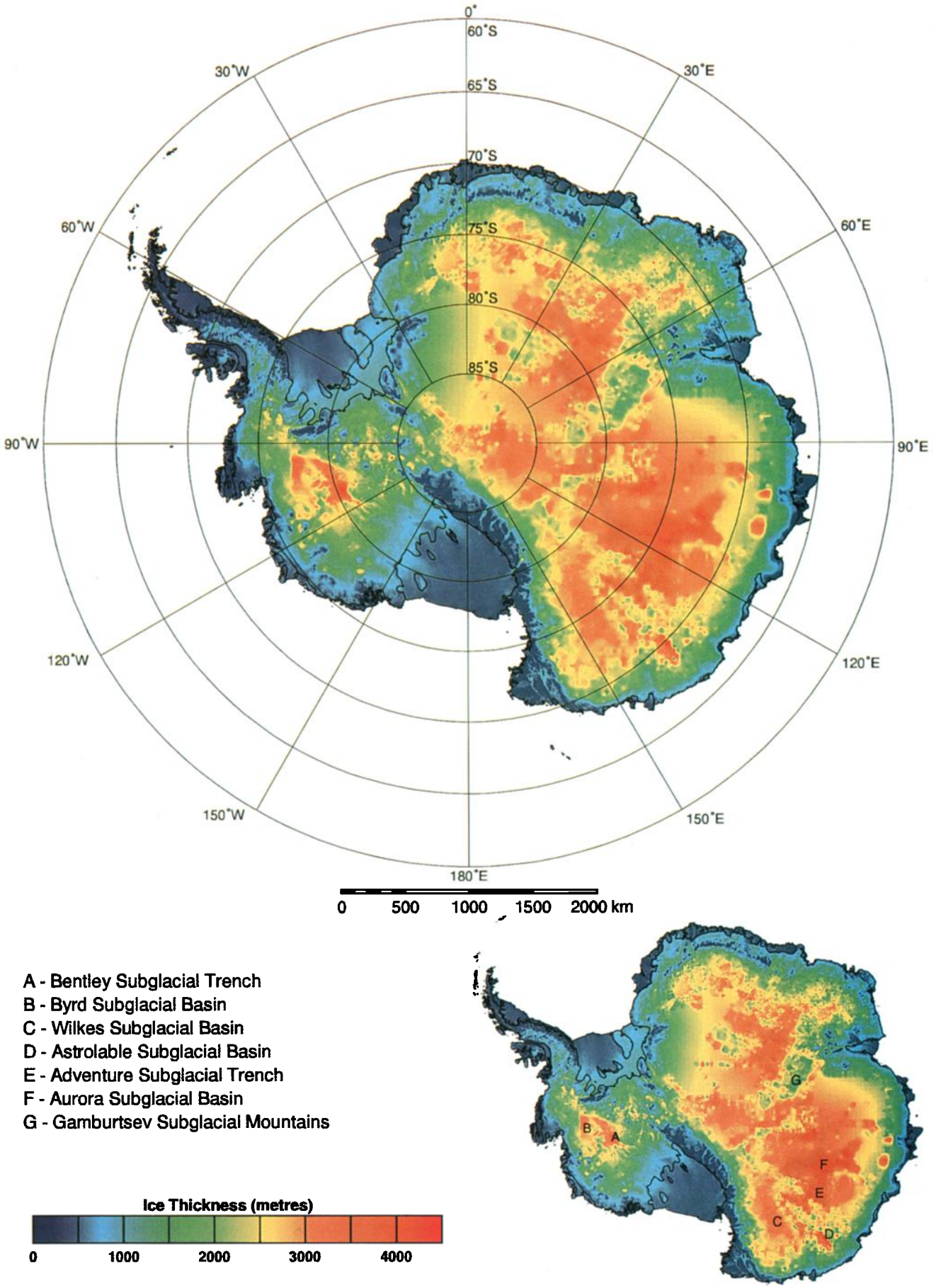

Plate 1. BEDMAP grid of Antarctic ice sheet thickness with coastline, and ice shelf fronts from the ADD.

duced maximum search distance of 50 km) to estimate the seabed topography.

3.4. Merging the Bed DEMS

The three bed DEMs (subglacial elevation, open-sea bathymetry, and sub-ice-shelf bathymetry) were merged into a composite grid by using the Hermite cubic function. The resulting composite model of bed topography for the region south of 60°S is a 1334 x 1334 data array with a grid spacing of 5 km; the model has a total elevation range of approximately 11,000 m. In addition to the orthometric DEM, which is referenced to the OSU91A geopotential model, we also constructed an ellipsoidal height DEM relative to the WGS84 ellipsoid by adding the geoidal-ellipsoid separation which ranges from -67 to +42 m [*Rapp et al.*, 1991].

3.5. Estimated Uncertainty in Final Bed DEM

The estimated uncertainty varies across the bed DEM according to the distribution of the original source data and the procedure used in its construction. We have evaluated both planimetric and vertical accuracy confidence limits for the bed DEM.

3.5.1. Horizontal accuracy. For the grounded ice sheet the horizonatal accuracy depends on both the Liu-DEM and the ice thickness grid. The Liu-DEM has an absolute positional accuracy of between 100 and 300 m [*Liu et al.*, 1999] except in some areas, such as the inland plateau, where the accuracy is around 10 km. As was outlined previously (see "Navigation"), the positional accuracy of the ice thickness data varies considerably according to the navigation methods used. While the GPS-navigated data are accurate to 100 m, much of the of older data collected have confidence limits of up to 5 km.

The positional accuracy of the bathymetric and sub-ice-shelf data is also variable. The satellite-derived gravity data have a horizontal resolution limit of 5-10 km in position [*Smith and Sandwell*, 1997]; the BCWS, around 100 m [*Schenke et al.*, 1998]; and the ETOPO-5 data, approximately 10 km. Where the sub-ice-shelf bathymetry is controlled by seismic data, the positional accuracy is similar to the ice thickness grid. We estimate that the horizontal accuracy of our bed DEM is between 200 m and 10 km.

3.5.2. Vertical accuracy. The absolute vertical accuracy of the bed DEM also varies across the model. By combining the confidence limits of the Liu-DEM (2-130 m) and the ice thickness grid (RMS error of 152 m for jackknife resample) we estimate the accuracy of the grounded ice sheet model to be generally between 150 and 300 m. In some mountainous regions, where the bed DEM uncertainty is greater, the vertical error is probably closer to 400 m. The vertical accuracy of the bathymetry data ranges from approximately 50 m for the BCWS to 250 m (satellite-derived gravity data) to around 500 m for ETOPO-5. For the majority of the sub-ice-shelf region it is difficult to estimate uncertainty, as the bed in these areas is only speculative. Where the model is controlled below the ice shelves, we estimate the vertical accuracy to be approximately 200 m. Overall, the vertical accuracy of the composite bed DEM is between 50 and 500 m.

4. Discussion

4.1. Principal Features of Ice Thickness Model

The quality and detail of the ice thickness model (Plate 1) reflect the density and distribution of the input data. In areas of closely spaced RES data (e.g., West Antarctica, Enderby Land, Kemp Land, and coastal Dronning Maud Land) the model resolves variation at spatial scales of around 15-20 km, while in more data-sparse regions the true horizontal resolution is more than 100 km. In several areas, where only a few measurements are available, the model contains isolated nodes of thick or thin ice. While these features may not reflect the regional ice thickness, they have been retained, as we have no reason to doubt their accuracy.

The thickest ice is located in the major subglacial basins. In West Antarctica, the Byrd Subglacial Basin and the Bentley Subglacial Trench are well defined (containing over 3000 m of ice). In East Antarctica, prominent features include the Wilkes Subglacial Basin, the Astrolabe Subglacial Basin, the Adventure Subglacial Trench, and the Aurora Subglacial Basin. The thickest ice observation (4776 m) is located in the Astrolabe Subglacial Basin. Relatively thick ice is also apparent in Enderby Land (between 75°S and 80°S and between 30°E and 60°E), an area which is far better delineated than in the SPRI Folio Series, because of the inclusion of considerable new Soviet and Russian data.

The frequency distribution of ice thickness values within the model (Figure 6) reveals a bimodal distribution with a peak around 400 m, corresponding to the ice shelves, and a secondary peak at ~2800 m, corresponding to the interior of the ice sheet. The minor, but significant, peak at ~20 m represents the moun-

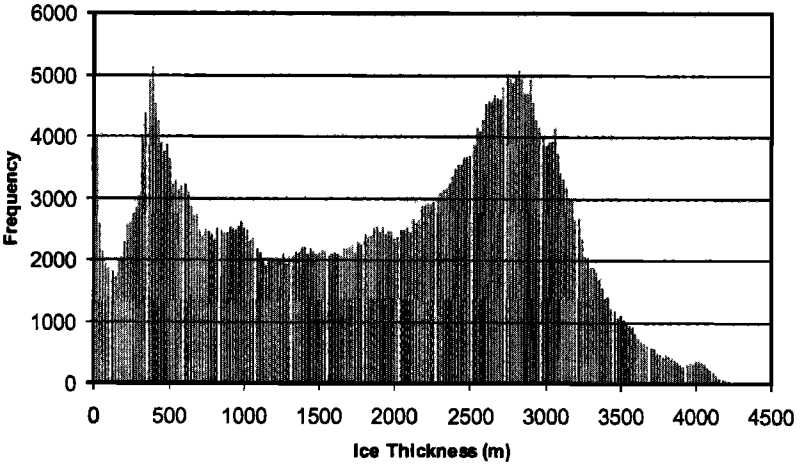

Figure 6. Ice thickness frequency distribution in the BEDMAP grid of Antarctic ice sheet thickness.

Table 4. Measured Properties of the Antarctic Ice Sheet From the 5-km Ice Thickness Grid[a]

Parameter	East Antarctica	West Antarctica	Total
Mean ice thickness, m	2146	1048	1856
Total volume including ice shelves, km^3	21.8×10^6	3.6×10^6	25.4×10^6
Grounded ice sheet volume, km^3	21.7×10^6	3.0×10^6	24.7×10^6
GIS volume above mean sea level, km^3	20.5×10^6	2.1×10^6	22.6×10^6
GIS volume below mean sea level, km^3	1.1×10^6	1.0×10^6	2.1×10^6
Sea level equivalent, m	52	5	57

[a]GIS, grounded ice sheet.

tainous regions and areas of exposed rock. The mean ice thickness across the entire grid is 1856 m, ~10% lower than the SPRI Folio Series estimate of 2160 m [*Drewry*, 1983b] but comparable to a recent estimate of 1903 m [*Huybrechts et al., 2000*]. The mean ice thickness of the grounded ice sheet is 2034 m, while for the ice shelves we determine a mean of 440 m.

The BEDMAP grids were used to determine the total volume of ice resident in the Antarctic ice sheet (Table 4). We compute a total volume of 25.4×10^6 km^3 for the entire ice sheet (ice sheet and ice shelves), which is close to early estimates of $24\text{-}26 \times 10^6$ km^3 [*Thiel*, 1962; *Vinnik et al.*, 1976]. The total volume from this compilation is, however, 15% less than the widely quoted 30.1 x 106 km^3 estimated from the SPRI Folio Series [*Drewry*, 1983b]. This offset was expected, as previous workers [*Bamber and Huybrechts*, 1996; *Huybrechts, et al.*, 2000] have found considerable uncertainty in the SPRI Folio Series estimate. Much of the uncertainty stems from the significant differences between the surface elevation distribution of the SPRI Folio map and improved elevation models derived from satellite altimetry.

Our derived volume for the Antarctic ice sheet is 4% lower than the most recent estimate of 26.4×10^6 km^3 [*Huybrechts et al.*, 2000] determined by using a 20-km ice thickness grid based on an updated version of the digitized SPRI Folio map. The reduction in mean ice thickness and ice volume is principally due to the higher topography in Enderby Land and Kemp Land, mapped for the first time by using Soviet and Russian data.

To determine the sea level equivalent of the ice volume, we calculated the total mass of the grounded ice sheet (assuming a mean density of 917 kg m^{-3}) and the mass of seawater required to fill the region below sea level if the ice sheet was removed (assuming a mean sea water density of 1028 kg m^{-3}). Given that 360 Gt of water is required to raise global sea level by 1 mm [*Jacobs et al.*, 1992], the total Antarctic ice sheet represents around 57 m of sea level rise, comprising 52 m for the East Antarctic ice sheet and 5 m for the West Antarctic ice sheet.

Although this calculation provides a substantial re-estimate of a widely quoted figure, around 73 m [*Robin*, 1986], and is lower than the most recent estimate, around 61 m [*Huybrechts et al.*, 2000] we cannot simply assume that this represents a realistic potential contribution to sea level rise. The calculation currently ignores second-order effects related to historical deglaciation (postglacial rebound, and alteration of the geoid surface after deglaciation), and steric effects of increased freshwater content of the world's oceans, etc.).

4.2. Principal Features of the Bed DEM

The morphology of the bed DEM (Plate 2) largely confirms that presented in the SPRI Folio Sheet 3 and from more recent published local surveys [*Allison et al.*, 1982; *Retzlaff et al.*, 1993; *Tabacco et al.*, 1998; *Blankenship et al.*, 2000; *Steinhage et al.*, 2000; *Damm*, 1996]. The present model, however, contains greater detail, is more justifiable and will be more easily updated than any previously published continental bed DEM.

Plate 2 confirms that East Antarctica and West Antarctica are morphologically distinct. East Antarctica is a largely contiguous landmass with a few broad basins, while West Antarctica is comprised of archipelagoes in discrete topographic units (Antarctic Peninsula, Ellsworth Mountains, Executive Committee and Flood Ranges, Whitmore Mountains, and the Ellsworth Land coast), which may represent distinct tectonic blocks. These blocks are separated by deep trenches, sometimes occupied by ice streams and outlet glaciers, that are more than 3000 m below sea level in places. This contrasts with the topography inland from Siple Coast, which is very smooth with modest ridges and troughs marking the location of the ice streams draining into the Ross Ice Shelf.

The topographic boundary between East Antarctica and West Antarctica which seemed clear in SPRI Folio Sheet 3 is no longer so obvious in Plate 2. There appears to be no direct connection between Thiel Trough and the troughs on the Siple Coast adjacent to the Trans-Antarctic Mountains. In East Antarctica, the elongated Wilkes Subglacial Basin, which extends along 145°E, is a dominant feature west of the Trans-Antarctic Mountains and extends offshore beyond the grounding line. The topography in Queen Mary Land and Wilhelm II Land (south of 80°S and between 120°E and 80°E) remains poorly mapped.

With the incorporation of previously unpublished Russian and Soviet RES data, the Gamburtsev Subglacial Mountains are more extensive than shown by SPRI Folio Sheet 3. Unfortunately, the widelyspaced flight lines (~50 km) still prevent us from being able to delineate individual ranges in this region. The highest elevation in the Gamburtsev Subglacial Mountains (2980 m) is ~1000 m below the ice sheet. Plate 2 shows more extensive rolling topography inland of Enderby Land compared with the SPRI Folio Sheet 3 and improved topographic definition in Dronning Maud Land, in particular north of 80°S, described in more detail by *Steinhage et al.* [2000]. Within the continental boundary itself the bed DEM has a total elevation range of over 7000 m with the highest point being Vinson Massif (4678 m) and the lowest in the Bentley Subglacial Trench (-2496 m).

5. Summary

We have established a database for the majority of ice thickness observations of the Antarctic ice sheet which will be of substantial utility to many branches of geoscience. The suite of 5-km grid digital topographic models for the Antarctic continent and its surrounds, produced from this database, provide a reliable

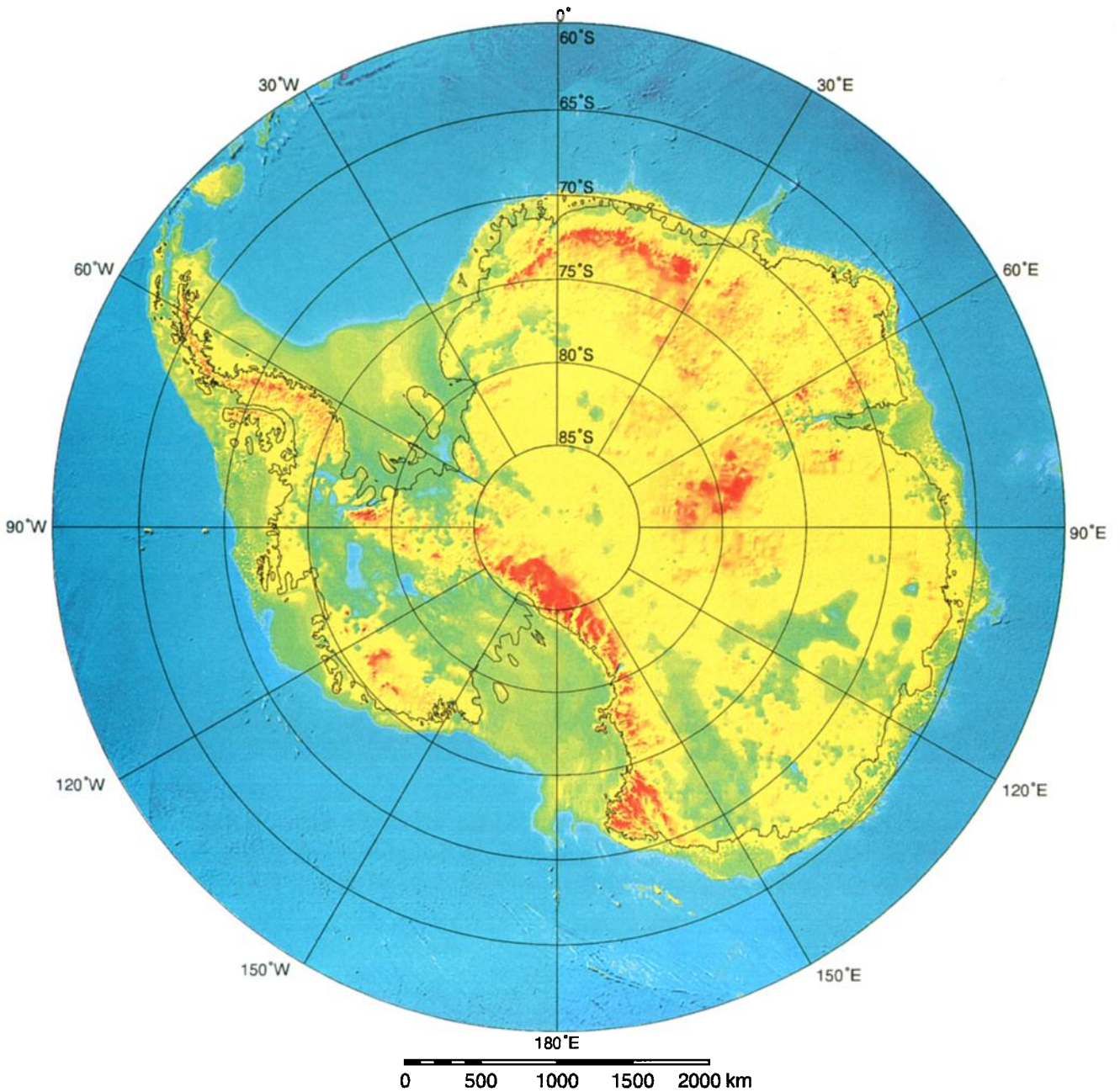

A - Executive Committee Range
B - Flood Range
C - Whitmore Mountains
D - Thiel Trough
E - Wilkes Subgacial Basin
F - Aurora Subglacial Basin
G - Gamburtsev Subglacial Mountains
H - Belgica Subglacial Highlands
I - Vostok Subglacial Highlands

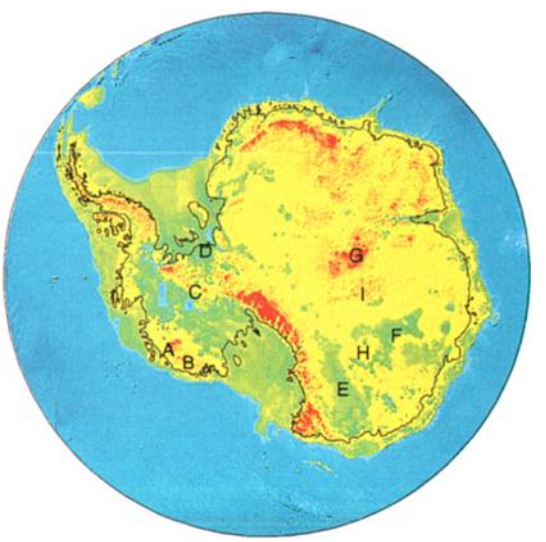

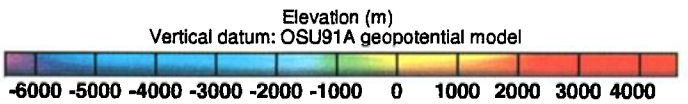

basis for ice sheet modeling and other continental-scale studies of Antarctica. The procedures used for data validation, processing, and gridding will enable relatively straightforward update of these products as more data become available. The present generation of models provide a unique insight into the subice topography beneath the Antarctic ice sheet. We have calculated the total volume of ice contained within the ice sheet to be 25.4 x 10^6 km^3. Further, the Antarctic ice sheet contains a volume of ice equivalent to 57 m of global sea level rise, 52 m for the East Antarctic ice sheet and 5 m for the West Antarctic ice sheet. The bed DEM, which includes the entire geosphere south of 60°S, provides an improved delineation of the boundary between East Antarctica and West Antarctica and sheds new light on the morphology of the contiguous East Antarctic landmass, much of which is buried below an average of 2500 m of ice.

6. BEDMAP Consortium

A. Lambrecht, H. Miller, U. Nixdorf, H. Oerter, and D. Steinhage, Alfred-Wegener-Institut für Polar-und Meeresforschung, Bremerhaven, Germany; I. F. Allison, M. Craven, I. D. Goodwin, J. Jacka, V. Morgan, A. Ruddell, and N. Young, Australian Antarctic Division, Hobart, Australia; P. Wellman, Australian Geological Survey Organisation, Canberra, Australia; A. P. R. Cooper, H. F. J.Corr, C. S. M. Doake, R. C. A. Hindmarsh, A. Jenkins, M. R. Johnson, P. Jones, E. C. King, M. B. Lythe, A. M. Smith, J. W. Thomson, M. R. Thorley, and D. G. Vaughan, British Antarctic Survey, Cambridge, UK; K. Jezek, B. Li, and H. Liu, Byrd Polar Research Center, Columbus, Ohio, M. Hideo, Communications Research Laboratory, Tokyo, Japan; V. Damm, Bundesanstalt für Geowissenschaften und Rohstoffe, Hanover, Germany; F. Nishio, Hokkaido University of Education, Japan; S. Fujita, Hokkaido University, Japan; P.Skvarca, Division Glaciologia - Instituto Antártico Argentino, Buenos Aires, Argentina; F. Remy, and L. Testut. Centre National de la Recherche Scientifique, Toulouse, France; J. Sievers, Bundesamt für Kartographie und Geodäsie, Frankfurt, Germany; A. Kapitsa, Moscow State University, Russia; Y. Macheret, Russian Academy of Sciences, Moscow, Russia; T. Scambos, National Snow and Ice Data Center, Boulder, Colorado; I. Filina, V. Masolov, and S. Popov, Ministry of Natural Resources of the Russian Federation-Polar Marine Geological Research Expedition, St. Petersburg, Russia; G. Johnstone, SCAR Working Group on Geodesy and Geographic Information, Canberra, Australia; B. Jacobel, St. Olaf College, Northfield, Minnesota; P. Holmlund, and J. Naslund, Stockholms Universitet, Stockholm, Sweden; S. Anandakrishnan, University of Alabama, Tuscaloasa; J. L. Bamber, R. Bassford, University of Bristol, Bristol, UK; H. Decleir, and P. Huybrechts, Université de Bruxelles, Bruxelles, Belgium; A. Rivera, Universidad de Chile, Santiago, Chile; N. Grace, University of Delaware, Newark; Delaware, G.Casassa, Universitad de Magallanes, Punta Arenas, Chile; I. Tabacco, Università degli Studi di Milano, Italy; D. Blankenship, and D. Morse, University of Texas at Austin; Austin, Texas,. Conway, T. Gades, and N. Nereson, University of Washington, Seattle, Washington, C. R. Bentley, and N. Lord, University of Wisconsin- Madison; Wisconsin, M. Lange, and H. Sandhäger, Westfälische Wilhelms-Universität, Münster, Germany.

Acknowledgments. The BEDMAP project was partially funded by the UK Natural Environment Research Council, SEEDCORN Initiative. Additional funding was provided from the British Antarctic Survey. The Scientific Committee on Antarctic Research (SCAR) provided financial assistance for the two BEDMAP workshops held in 1996 and 1999. The authors thank M. R. Thorley for assistance in the project.

References

Ageta, Y., T. Kikuchi, and K. Kamiyama, Glaciological research program in East Queen Maud Land, East Antarctica, part 5, 1985, *JARE Data Rep. 125*, 71 pp., Nat. Inst. of Polar Res., Tokyo, 1987.

Allison, I. F., R. Frew, and I. Knight, Bedrock and ice surface topography of the coastal region of Antarctica between 48 and 64*Polar Rec., 21*, 241-252, 1982.

Anandakrishnan, S., D. D. Blankenship, R. B. Alley, and P. L.Stoffa, Influence of subglacial geology on the position of a West Antarctic ice stream from seismic observations, *Nature, 394*, 62-65, 1998.

Angrisano, G., Hydrographic surveying and nauticalcharting: A coordinated effort of the International Hydrographic Organization (IHO), *Int. Hydrogr. Rev., 72*, 69-77, 1995.

Autenboer, T. V., and H. Decleir, Glacier discharge in the Sor Rondane, a contribution to the mass balance ofDronning Maud Land, Antarctica, *Z. Gletscherk. Glazialgeol., 14*, 1-16, 1978.

Bamber, J. L., and R. A. Bindschadler, An improved elevation dataset for climate and ice-sheet modeling: Validation with satellite imagery, *Ann. Glaciol., 25*, 439-444, 1997.

Bamber, J. L., and P. Huybrechts, Geometric boundary conditions for modeling the velocity field of the Antarctic ice sheet,*Ann. Glaciol.*, 23, 364-373, 1996.

Bamber, J. L., S. Ekholm, and W. Krabill, The accuracy of satellite radar altimeter data over the Greenland ice sheet determined from airborne laser data, *Geophys. Res. Lett., 25*, 3177-3180, 1998.

Bamber, J. L., D. G. Vaughan, and I. Joughin, Widespread complex flow in the interior of the Antarctic ice sheet,*Science, 287*, 1248-1250, 2000.

Behrendt, J. C., Geophysical andglaciological studies in the Filchner Ice Shelf area of Antarctica, *J. Geophys. Res., 67*, 221-234, 1962.

Bentley, C. R., The structure of Antarctica and its ice cover,in *Research in Geophysics*, vol. 2, *Solid Earth and Interface Phenomena*, edited by H. Odishaw, pp. 335-389, MIT Press, Cambridge, Mass., 1964.

Bentley, C. R., Antarctic ice streams: A review,*J Geophys. Res., 92*, 8843-8858, 1987.

Blankenship, D. D., D. L. Morse, C. A. Finn, R. E. Bell, M. E. Peters, S. D. Kempf, S. M. Hodge, M. Studinger, J. C. Behrendt, and J. M. Brozena, Geologic controls on the initiation of rapid basal motion for the ice streams of the southeastern RossEmbayment: A geophysical perspective including new airborne radar sounding and laser altimetry results, in *The West Antarctice Ice Sheet: Behavior and Environment, Antarct. Res. Ser.*, vol. 77, edited by R. B. Alley and R. Bindschadler, AGU, Washington, D. C., 2000.

British Antarctic Survey, (BAS), Scott Polar Research Institute, World Conservation Monitoring Centre, 1993. *Antarctic digital database (User's Guide and Reference Manual)*, Scientific Committee on Antarctic Research, Cambridge, xi, 156 pages.

Budd, W., The dynamics of the Amery Ice Shelf, *J. Glaciol., 6*, 335-358, 1966.

Budd, W. F., M. J. Corry and T. H. Jacka, Results from the Amery Ice Shelf project, *Ann. Glaciol., 3*, 36-41, 1982.

Budd, W. F., D. Jenssen, and I. N. Smith, A three-dimensional time-dependent model of the West Antarctic ice sheet, *Ann. Glaciol., 5*, 29-36, 1984.

Canadian Hydrographic Office, General Bathymetric Chart of the Oceans (GEBCO), 5th ed., Hydrogr. Chart Distrib. Off., Ottawa, Ont., 1981.

Casassa, G., and I. M. Whillans, Decay of surface topography on the Ross Ice Shelf, Antarctica, *Ann. Glaciol., 20*, 249-253, 1994.

Casassa, G., R. Carvallo, C. Cardenas, B. Jelinic, and A. Rivera, Performance of a snowmobile-based radio echo sounding system at Patriot Hills, Antarctica, in *Proceedings of the VIII SCALOP*

Plate 2. BEDMAP grid of bed elevation for the Antarctic continent and surrounding ocean. Assumed illumination is from the northwest. Shading is computed by using a vertical exaggeration of 40, but shadows are not included. The grounding line/coastline are taken from the ADD.
Sources, survey types and dates for ice thickness data collected over Antarctica and compiled in the BEDMAP database. The legend for the survey type is as follows: A - airborne Radio- Echo Sounding (RES), O - over-snow RES, S - seismic, G - gravity, B - borehole.

Symposium, pp. 93-101, 193pp, Standing Committee of Antarctic Logistic Operators (SCALOP), Conception, Chile, 1998.

Crary, A. P., E. F. Robinson, H. F. Bennet, and W. W. Boyd, *Glacial Studies of the Ross Ice Shelf, Antarctica, IGY Glaciology Rep.* American Geographical Society, New York, *Ser.*, Number 6, 1962.

Cressie, M., and D. M. Hawkins, Robust estimation of thevariogram, *Math. Geol.*, *12*, 115, 1980.

Damm, V., Subice morphology deduced from radio-echo soundings (RES) in the area between David and Mawson Glaciers, Victoria Land, *Geol. Jahrb.*, *B89*, 321-331, 1996.

Dieterle, G., and E. Peterschmitt, Sondages seismiques en Terre de la Reine Maud, *Mem. 13* p.101, Acad. R. des Sci. d'Outre-Mer, Classe des Sci. Tech., Brussels, 1964.

Drewry, D. J., Comparison of electromagnetic and seismic-gravity ice thickness measurements in East Antarctica, *J. Glaciol.*, *15*, 137-150, 1975.

Drewry, D. J., The surface of the Antarctic ice sheet, in *Antarctica: Glaciological and Geophysical Folio,* Scott Polar Res. Inst., Cambridge, England, U.K., 1983a.

Drewry, D. J., Antarctic ice sheet thickness and volume, in*Antarctica: Glaciological and Geophysical Folio,* Scott Polar Res. Inst., Cambridge, England, U.K., 1983b.

Drewry, D. J., and S. R. Jordan, The bedrock surface of Antarctica, in *Antarctica: Glaciological and Geophysical Folio,* Scott Polar Res. Inst., Cambridge, England, U.K., 1983.

Englehardt, H., and J. Determann, Borehole evidence for a thick layer of basal ice in the central regionof Ronne Ice Shelf, *Nature*, *327*, 318-319, 1987.

Fox, A. J., and A. P. R. Cooper, Measured properties of the Antarctic ice sheet derived from the SCAR Antarctic Digital Database, *Polar. Rec.*, *30*, 201-206, 1994.

Gades, A. M., C. F. Raymond, H. Conway, and R. W. Jacobel, Bed properties of Siple Dome and adjacent ice streams, West Antarctica, inferred from radio echo-sounding measurements, *J. Glaciol.*, *46* (152), 88-94, 2000.

Higham, M., M. Reynolds, A. Brocklesby, and I. Allison, Ice radar digital recording, data processing, and results from the Lambert Glacier basin traverses, *Terra Antarct.*, *2*(1), 23-32, 1995.

Hoppe, H., and F. Thyssen, Ice thickness and bedrock elevation in western Neuschwabenland and Berkner Island, Antarctica, *Ann. Glaciol.*, *11*, 42-45, 1988.

Huybrechts, P., D. Steinhage, F. Wilhelms, and J. L. Bamber, Balance velocities and measured properties of the Antarctic ice sheet from a new compilation of gridded data for modeling, *Ann. Glaciol.*, *30*, in press, 2000.

Jacobel, R. W., T. A. Scambos, C. F. Raymond, and A. M. Gades, Changes in the configuration of ice stream flow from the West Antarctic ice sheet, *J. Geophys. Res.*, *101*, 5499-5504, 1996.

Jacobs, S. S., H. H. Helmer, C. S. M. Doake, A. Jenkins, and R. M. Frolich, Melting of ice shelves and the mass balance of Antarctica, *J. Glaciol.*, *38*, 375-387, 1992.

Jankowski, E. J., and D. J. Drewry, The structure of West Antarctica from geophysical studies, *Nature*, *291*, 17-21, 1981.

Jenkins, A., and C. S. M. Doake, Ice-ocean interaction onRonne Ice Shelf, Antarctica, *J. Geophys. Res.*, *96*, 791-813, 1991.

Johnson, M. R., and A. M. Smith, Seabed topography under the southern and western Ronne Ice Shelf, derived from seismic surveys, *Antarct. Sci.*, *9*, 201-208, 1997.

Kapitsa, A. P., New data on ice thickness in the central regions of Antarctica, *Sov. Antarct. Exped. Inf. Bull.*, Engl. Transl. *2*, 247-250, 1964.

Kapitsa, A. P., and O. G. Sorokhtin, On errors in interpretation of reflection seismic shooting in the Antarctic, Int. Union ofGeods. and Geophys., Assoc. Int. des Sci. Hydrol., Gentbrugge, Belgium, 1963.

Keller, M. A, M. T. Diaz, and P. Skvarca, *Estudio Geofisico en el Sector Norte de la Peninsula Antartica y Barrera de Hielos Larsen,* pp 81-90,. edited by A. Louro, M. A. Van Zele, and I. Velasco, Centro Latinoamericano de Fisica, Buenos Aires, 1990.

Kurinin, R. G., and N. D. Aleshkova, Korennoj relief Zemli Enderby, Zemli Mak-Robertsona i Zemli princessi Elizaveti v Vostochnoj Antarctide (Subice relief of Enderby Land, Mac. Robertson Land and Princess Elizabeth Land in East Antarctica), *Antarctica, 26,* 62-65, 1987.

Liu, H. X., K. C. Jezek, and B. Li, Development of Antarctic DEM by integrating cartographic and remotely sensed data: A GIS-based approach, *J. Geophys. Res.*, *104*, 23,199-23,213, 1999.

Macheret, Y. Y., M. Y. Moskalevsky, J. C. Simoes, and L. Ladouch, Study of King George Island ice cap, South Shetland Islands, Antarctica using radio-echo sounding and SPOT, ERS-1 SAR satellite images, *Eur. Space Agency, Spec. Publ.*, ESA SP 405, 249-255, 1997.

Morgan, V. I., Oxygen isotope evidence from bottom freezing on the Amery Ice Shelf, *Nature, 238*, 393-394, 1972.

Morgan, V. I., and W. F. Budd, Radio-echo sounding of the Lambert Glacier basin, *J. Glaciol.*, *15*, 103-111, 1975.

Morgan, V. I., T. H. Jacka, G. J. Akerman, and A. L. Clarke, Outlet glacier and mass-budget studies in Enderby, Kemp and Mac-Robertson Lands, Antarctica, *Ann. Glaciol.*, *3*, 204-210, 1982.

National Geophysical Data Center, ETOPO-5bathymetry/topography Data Announce. *88-MGG-02,* Natl. Oceanic and Atmos. Admin., U.S. Dep. of Commer., Boulder, Colo., 1988.

Nishio, F., H. Ohmae, and M. Ishikawa, Glaciological research program in east Queen Maud Land, East Antarctica, part 3, 1982, *JARE Data Rep.*, *10*, 110, pp. 36, Nat. Inst. of Polar Res., Tokyo, 1986.

Nishio, F., S. Uratsuka, and H. Ohmae, Bedrock topography, sheet 8, in *Antarctica: East Queen Maud Land Enderby Land Glaciological Folio,* Nat. Inst. of Polar Res., Tokyo, Japan, 1997.

Pattyn, F., and H. Decleir, Subglacial topography in the central Sor Rondane Mountains, East Antarctica: Configuration andmorphometric analysis of valley cross profiles, *Antarct. Rec.*, *39*, 1-24, 1995.

Payne, A. J., Self-organization in the thermomechanical flow of ice sheets, *J. Geophys. Res.*, *102*, 12,219-12,233, 1997.

Payne, A. J., A thermomechanical model of ice flow in West Antarctica, *Clim. Dyn.*, *15*, 115-125, 1999.

Pozdeev, V. S., and R. G. Kurinin, Novie dannie o morphologii ledovoj tolschi irelefe podlednogo loga i morskogo dna v juzhnoj chasti basseina morja Uedella (Zapadnaja Antarctida) (New data about ice thickness, subice relief and bathymetry of south part Weddell Sea basin (West Antarctica)), *Antarctica, 26,* 66-71, 1987.

Rapp, Y., M. Wang, and N. K. Pavlis, The Ohio State 1991 geopotential and sea surface harmonic coefficient models, *Rep. 410*, Dep. of Geod. Sci. and Surv., Ohio State Univ., Columbus, Ohio, 1991.

Retzlaff, R., N. Lord, and C. R. Bentley, Airborne radar studies: Ice Streams A, B and C, West Antarctica, *J. Glaciol.*, *39*, 495-506, 1993.

Robin, G. de Q., Radio-echo sounding applied to the investigation of the ice thickness and sub-ice relief of Antarctica, in *Antarctic Geology and Geophysics*, pp. 675-682, Universitetsforlaget, Oslo, 1971.

Robin, G. de Q., Changing sea level: Projecting the rise in sea level caused by warming of the atmosphere, in *The Greenhouse Effect, Climatic Change and Ecosystems (SCOPE 29),* edited by B. Bolin, B. R. Doos, J. Jager, and R. A. Warrick, pp. 323-359, John Wiley, New York, 1986.

Robin, G. de Q., C. W. M. Swithinbank, and B. M. E. Smith, Radio echo exploration of the Antarctic ice sheet, in *International Symposium on Antarctic Glaciological Exploration,* pp. 97-115, U.S. Cold Regions Res. and Eng. Lab., Hanover, N. H., 1973.

Rothlisberger, H., Seismic exploration in cold regions, in*Cold Regions Engineering*, part II, U.S. Cold Regions Res. and Eng. Lab., Hanover, N. H., 1972.

Schenke, H. W., S. Dijstra, F. Neiderjasper, T. Schone, H. Hinze, and B. Hoppman, The new bathymetric charts of the Weddell Sea: AWI BCWS, in *Ocean, Ice and Atmosphere: Interactions at the Antarctic Continental Margin, Antarct. Res. Ser.*, vol. 75, edited by S. Jacobs and R. Weiss, pp. 371-380, AGU, Washington, D. C., 1998.

Scientific Committee on Antarctic Research Working Group on Geodesy and Cartography, Standard symbols for use on topographic maps of Antarctica, Div. of Natl. Mapp., Canberra, 1961.

Shabtaie, S., I. M. Whillans, and C. R. Bentley, The morphology of Ice Streams A, B, and C, West Antarctica, and their environs, *J. Geophys. Res.*, *92*, 8865-8883, 1987.

Sichoix, L., and A. Bonneville, Prediction of bathymetry in French Polynesia constrained by shipboard data, *Geophys. Res. Lett.*, *23*, 2469-2472, 1996.

Smith, A. M., and C. S. M. Doake, Seabed depths at the mouth of Rutford Ice Stream, Antarctica, *Ann. Glaciol.*, *20*, 353-356, 1994.

Smith, W. H. F., On the accuracy of digital bathymetry data, *J. Geophys. Res.*, *98*, 9591-9603, 1993.

Smith, W. H. F., and D. T. Sandwell, Bathymetric prediction from dense satellite altimetry and sparse shipboard bathymetry, *J. Geophys. Res.*, *99*, 21,803-21,824, 1994.

Smith, W. H. F., and D. T. Sandwell, Global sea floor topography from satellite altimetry and ship depth soundings, *Science*, *277*, 1956-1961, 1997.

Steinhage, D., U. Nixdorf, U. Meyer, and H. Miller, New maps of the ice thickness and subglacial topography in Dronning Maud Land, Antarctica, determined by means of airborne radio echo sounding, *Ann. Glaciol.*, *29*, 267-272, 2000.

Tabacco, I. E., A. Passerini, F. Corbelli, and M. Gorman, Determination of the surface and bed topography at Dome C, East Antarctica, *J. Glaciol.*, *44*, 185-191, 1998.

Thiel, E. C., The amount of ice on planet Earth, in *Antarctica Research: The Matthew Fontaine Maury Memorial Symposium, Geophys. Monogr. Ser.*, vol. 7, edited by H. Wexler et al., pp. 172-175, AGU, Washington, D. C., 1962.

Thyssen, F., and K. Grosfeld, Ekstrom Ice Shelf, Antarctica, *Ann. Glaciol.*, *11*, 180-183, 1988.

Tichelaar, B. W., and L. J. Ruff, How good are our best models? Jackknifing, bootstrapping, and earthquake depth, *EOS, Trans. AGU*, *70*, 593-605, 1989.

Vaughan, D. G., and J. L. Bamber, Identifying areas of low-profile ice and outcrop damming in the Antarctic ice sheet by ERS-1 satellite altimetry, *Ann. Glaciol.*, *27*, 1-6, 1998.

Vaughan, D. G., J. Sievers, C. S. M. Doake, G. Grikurov, H. Hinze, V. S. Pozdeev, H. Sandhager, H. W. Schenke, A. Solheim, and F. Thyssen, Map of subglacial and seabed topography, scale 1:2,000,000, Filchner-Ronne-Schelfeis/Weddell Sea, Antarkis, Inst. fur Angewandte Geod., Frankfurt, Germany, 1994.

Vaughan, D. G., J. Sievers, C. S. M. Doake, H. Hinze, D. R. Mantripp, V. S. Pozdeev, H. Sandhager, H. W. Schenke, A. Solheim, and F. Thyssen, Subglacial and seabed topography, ice thickness and water column thickness in the Vicinity of Filchner-Ronne-Schelfeis, Antarctica, *Polarforschung*, *64*, 75-88, 1995.

Vinnik, A. B., B. V. Dubovsky, Ja. P. Koblents, and E. C. Korotkevich, New data on principal morphometrical characteristics of Antarctica, *Sov. Antarct. Exped. Inf. Bull.*, Engl. Transl., *93*, 13-18, 1976.

von Frese, R. R. B., L. Tan, J. W. Kim, and C. R. Bentley, Antarctic crustal modeling from the spectral correlation of free-air gravity anomalies with the terrain, *J. Geophys. Res.*, *104*, 25,275-25,296, 1999.

Walker, D. J., Wilkes geophysical surveys, Antarctica 1962, *Rec. 1966/129*, Bur. of Miner. Resour., Geol. and Geophys., 51 pp., Canberra, Australia, 1966.

Young, N. W., I. D. Goodwin, N. W. J. Hazelton, and R. J. Thwaites, Measured velocities and ice flow in Wilkes Land, Antarctica, *Ann. Glaciol.*, *12*, 192-197, 1989.

D. G. Vaughan, British Antarctic Survey, High Cross, Madingley Road, Cambridge, England. U.K.

(Received June 29, 2000; revised November 21, 2000; accepted November 30, 2000.)